Journal of Materials Chemistry B

Accepted Manuscript

ROYAL SOCIETY OF CHEMISTRY

www.rsc.org/materialsB

Cite this: DOI: 10.1039/c0xx00000x

www.rsc.org/xxxxxx

ARTICLE TYPE

A proton-responsive ensemble using mesocellular foam supports capped with N, O-carboxymethyl chitosan for controlled release of bioactive proteins

Qi Gan,[a,b,c] Jiaoyang Zhu,[a,b] Yuan Yuan,*[a,b] Honglai Liu,[c] Yihua Zhu,[b] Changsheng Liu*[a,b]

Received (in XXX, XXX) Xth XXXXXXXXX 20XX, Accepted Xth XXXXXXXXX 20XX
DOI: 10.1039/b000000x

A novel pH-responsive mesocellular foam-based nanocarrier was fabricated by covalent assembly of a water-soluble N, O-carboxymethyl chitosan *via* crosslinking of GPTMS. The delivery systems show excellent protein loading with programmable release in acid environment. Moreover, the released proteins still preserve their conformation and biological activity.

Tremendous researches studying the therapeutic potential of peptides and proteins have introduced a large number of protein medicines to the pharmaceutical industry, such as aldesleukin, synthetic insulin, bone morphogenic protein, and others.[1] The successful application of these biologic entities depends on ability to successfully preserve their function and activity in what is often unnatural environment. Nowadays, formulating protein/peptides into polymer microcapsules may represent the most commonly used method to improve the protein stability against enzymatic degradation and prolong the therapeutic effect.[2] However, organic solvents widely used in preparation of such traditional delivery system often lead to the changes of the secondary structures and thus undermine biological activity of the proteins. Therefore, biocompatible micro- and nano-carrier delivery systems with excellent function to preserve the structures and bioactivities of inner peptides or proteins are highly desired.[3]

Recently, entrapment of protein in mesopore has aroused great attention in the field of electrics, catalysis, etc.[4] Previous researches have recognized that mesoporous structure with tunable pore size similar to the macromolecules can supply a restrained and interactive microenvironment to preserve or enhance the biological activity and stability of proteins.[5] In particular, mesocellular silica foam (MCF), which is composed of three-dimensional ultra-large spherical pores (>20 nm) interconnected by smaller windows, and have high specific surface areas and volumes, should be very suitable materials for protein immobilization.[6] Furthermore, the silanol-containing surfaces of MCF that can be easily functionalized to make it possible to fabricate delivery systems with ideal "zero release" and physical or chemical stimuli-induced controlled release simultaneously. As far as the stimuli are concerned, pH-triggered catch and release of cargo is particularly attractive on account of that it can make use of physiological gradients of pH.[7] For instance, the pH value is about 7.35 -7.45 in bloodstream, approximately 5.5 in endosomes, while extracellular pH in the tissue at early stages of wound healing, inflamed tissue, or tumors, may range from 5.5 to 6.9.[8]

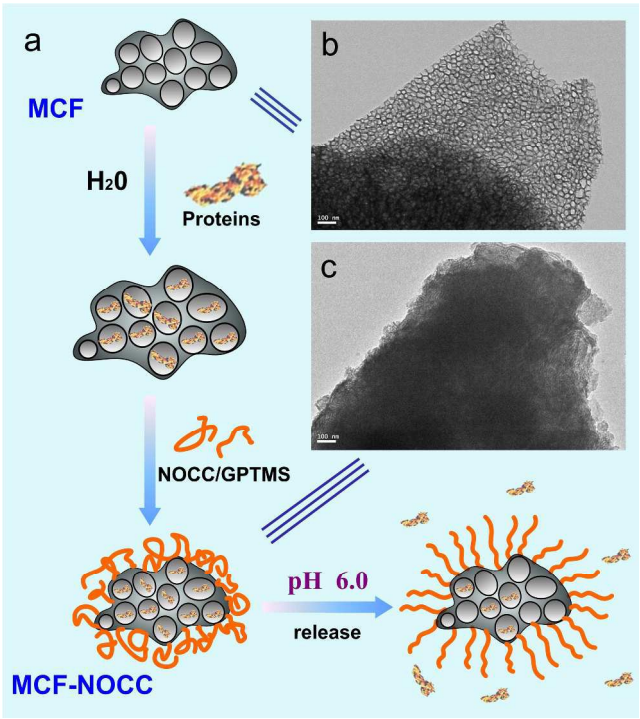

Fig. 1 (a) Schematic of synthesis of MCF-NOCC and controlled release of protein from MCF-NOCC, inset are TEM images of MCF (b) and MCF-NOCC (c). Scale bar = 100 nm.

Herein, a nanoscopic pH-responsive MCF-based protein delivery system was fabricated for protein delivery. N,O-carboxymethyl chitosan (NOCC), a water-soluable chitosan derivative with effects of the ionic functional groups and pH-sensitive behavior,[9, 10] was chosen to fabricate onto the outlet of the MCF surface not only as a "gate-like" switch to achieve pH-responsive release, but also as a protective agent for entrapped proteins away from the external environment. What is more, the excellent water solubility makes it possible to attach NOCC in neutral aqueous solutions, which is beneficial to protect the drug/protein previously entrapped in the matrix from degradation or denaturation. Additionally, the preparation process of such a

delivery system is simple and in a completely mild aqueous environment.[11] As shown in Fig. 1a, the MCF with ultra-large spherical pores and high pore volumes was first prepared and bioactive proteins were then loaded in the solution of MCF for a period time. After that, NOCC was functionalized onto the surface of MCF via the cross-linking of glycidoxypropyltrimethoxysilane (GPTMS). Under physiological conditions, proteins were encapsulated in the ultra-large spherical cells because of the coverage of NOCC at the pore windows. At the acidifying disease sites or endosomes environment, the conformation and structure of NOCC were changed into dispersing states and the encapsulated proteins were then released to the external environments. The choice of NOCC-functionalized MCF provides an all-aqueous environment, thus two major problems in formulation of protein delivery systems, i.e., preservtion the bioactivity of proteins and precise control over release of proteins, can be addressed.

NOCC was first synthesized and characterized. The FTIR spectrum (Fig. S1) and the ^{1}H NMR spectrum results (Fig. S2) indicated that the carboxymethyl substituents were successfully introduced on the amino and hydroxyl sites of the chitosan structure. Next, NOCC was then coated onto the surface of MCF via the cross-linking of GPTMS (Scheme S1). The morphologies and microstructures of the prepared MCF and MCF-NOCC were clearly revealed by TEM. As shown in Fig. 1b, MCF materials owned an obvious porous structure, which composed of uniformly sized, ultra-large spherical cells that are interconnected by uniform narrow windows to create a continuous 3D pore system. After being coated by NOCC, the TEM image of MCF materials showed clear wrapping of the NOCC on the outer surface of MCF (Fig. 1c). It is demonstrated that the NOCC is coated onto the outer surface of MCF owing to its extremely large molecular size (~ 3.0 × 10^4 Da) and its complex conformation, making it difficult to go inside the spherical cells across the narrow windows.

It is interesting to note from Fig. 2a that these MCFs displayed a significant spherical agglomerate state in particle morphology, and the particle size mainly distributed over 1 - 2 μm. The high-magnification SEM image in Fig. 2b clearly illustrated the high porosity and ultra-large pore size of the prepared MCF microparticles. Furthermore, it is shown that some MCF microparticles were aggregated in the form of “dimers” or “trimers” consisting of two or three spherical particles. As shown in Fig. 2c, the functionalization of NOCC onto the surface of MCF did not have significant effect on the particle size and morphology of spherical microparticles. But the high-magnification SEM image (Fig. 2d) showed almost all ultra-large pores on the outer surface of particles were disappeared. From Fig. 2e, the FTIR spectra of both MCF and MCF-NOCC all displayed absorption bands at about 802 cm^{-1} and 1091 cm^{-1}, which can be assigned to the characteristic peaks of stretching vibrations of the Si-O bond. However, the specific band at 2936 cm^{-1} attributable to the vibration of C-H bond was only observed in the spectra of MCF-NOCC. The TG of MCF-NOCC (Fig. 2f) showed ~15% weight loss between 225 and 350 °C, while the sample of MCF was displayed about 1% weight loss in this temperature range, due to the degradation of surface organic groups-NOCC. Degradation due to the breaking of main chain of NOCC was observed above 300 °C. The surface analysis of MCF and MCF-NOCC was performed by N_2 adsorption isotherms, which were shown in Fig. 2g and Table S1. After modified with NOCC, the BET surface area was decreased from 600 $m^2 \cdot g^{-1}$ of MCF to 53.1 $m^2 \cdot g^{-1}$, the pore volume also decreased from 2.12 $cm^3 \cdot g^{-1}$ to 0.21 $cm^3 \cdot g^{-1}$, and the pore size of particles decreased to also zero. MCF and MCF-NOCC all had good biocompatibilities, which is an important character for a drug/protein delivery material (Fig. S3). Moreover, they exhibited a little higher ALP activity than control, which means the two carriers facilitate the osteoblast differentiation of BMSCs (Fig. S4).

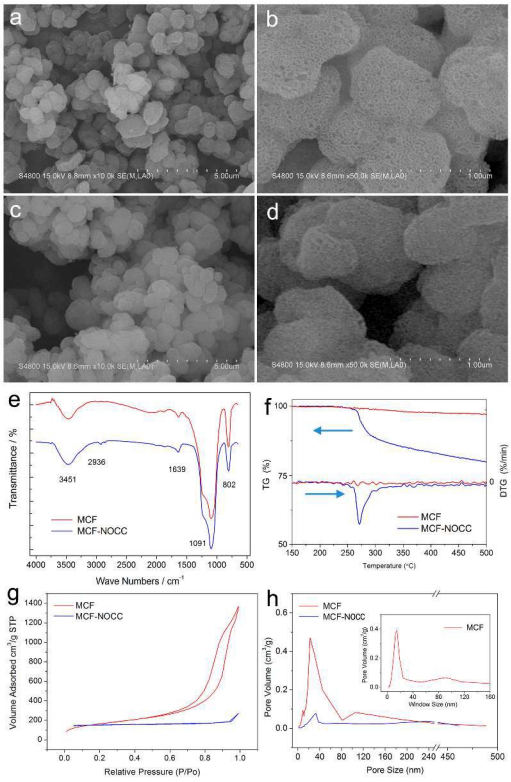

Fig. 2 SEM of MCF (a & b) and MCF-NOCC (c & d), magnification of (a) and (c) are ×10^4, magnification of (b) and (d) are 5×10^4. The FTIR spectra (e), thermogravimetric analysis (f) and nitrogen adsorption / desorption isotherms (g) of prepared MCF and MCF-NOCC. (h) is pore size distribution of MCF and MCF-NOCC, the inset of (h) is window size of MCF materials.

To demonstrate the effectiveness of our designed system, we selected two kinds of proteins with different properties and molecular weight as model protein. BSA (molecular mass 67 000 D) is a large protein with negative charge at pH 6.0 - 7.4, while BMP-2 (molecular mass 26 000 D) is a much smaller protein with three-dimension of 7 nm × 3.5 nm × 3 nm and is positive charged at pH 6.0 - 7.4.[12] Especially, as one of the most notable cytokines to enhance bone formation, the highly efficient delivery of BMP-2 in a bioactive form is a major challenge in the field of drug delivery systems. With BSA as example, as shown in Fig. S5 and Table S1, the total pore volume and pore size were considerably decreased, ca. 40% for MCF-BSA, as a consequence of the successful loading of BSA in the pores.

As shown in Fig. 3a, the total percent of BSA loading was 43% and 53% for MCF and MCF-NOCC, and the BMP-2 loading percent was 77% and 65% for MCF and MCF-NOCC, respectively. Given that the surface of MCF is rich in silanol groups (pK_a around 3), the MCF is negatively charged (Zeta potential -27.3 mV), whereas the NOCC, functionalized onto the surface of MCF, is rich in carboxymethyl groups and amino groups (with a slightly positive charge). During the process of capping MCF, there exist two processes: protein adsorbed on the NOCC and capped onto the surface of MCF, and protein leak out of the pores of MCF. For negatively-charged BSA protein (pI ~ 4.7), the favorable electrostatic interactions between the NOCC and protein may facilitate the adsorption of protein on the NOCC and increase the loading amount. However, for positively-charged BMP-2, the weak electrostatic interactions between NOCC and BMP-2 resulted in more BMP-2 release from the system than that adsorbed onto the NOCC, leading to the reduction of the loading amount of BMP-2 after capped of NOCC. Considering that the BMP-2 is very expensive, in this study, the protein concentration for loading was kept at a relatively low concentration of 5 mg/mL, which led to a low content of protein in the final MCF-NOCC system. Further study confirmed that it can be increased by increasing the concentration of the protein.

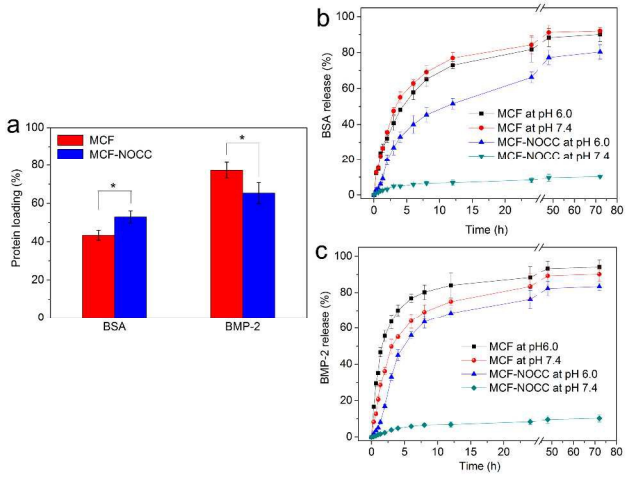

Fig. 3 (a) The loading percentages of BSA and BMP-2 by MCF and MCF-NOCC. The release profiles of BSA (b) and BMP-2 (c) from MCF and MCF-NOCC at pH 6.0 or pH 7.4 in PBS solution. (n = 3, $p < 0.05$)

Subsequently, the release profiles of BSA and BMP-2 from MCF and MCF-NOCC at room temperature were studied with BCA Kit assay in supernatant after separation of the solid by centrifuge. Two release media were prepared at two different pH values (7.4 and 6.0) to mimic the pH value in the normal body fluids and pathological changed position. As shown in Fig. 3b, MCF showed a burst release of BSA in the initial 6 h at both pH 6.0 and pH 7.4. It is to be noted that more than 80% BSA protein released from MCF in initial 24 h and showed no change irrespective of the pH. This result is due to the weak interaction between negatively charged MCF and negatively charged BSA and the protein release is controlled by mere diffusion. Furthermore, the diffused release of BSA from MCF-NOCC was also occurred at pH 6.0. Previous researches[9, 11] have demonstrated that loop or tail conformations of the charged NOCC chain depended on the pH value of the surrounding environment. The tail conformation can be found by protonation of primary amino groups when the pH is below its isoelectric point, while the NOCC shows loop conformation when the pH value is larger than the isoelectric point. Therefore, when the pH value of release solution is 6.0, the switch of this pH-responsive protein delivery system is open because the NOCC exhibits the tail conformation. Additionally, the release of BSA from MCF-NOCC was a little slower than that from MCF. This may be attributed to the increased steric hindrance via the coating of NOCC onto the surface of spherical pores. In contrast, at pH 7.4, MCF-NOCC shows zero or no release for the entire release time. This is due to the closing of NOCC switch via the change of conformation. The release of BMP-2 from MCF and MCF-NOCC at pH 6.0 and pH 7.4 was displayed in Fig. 3c. The release behavior of BMP-2 is similar to the release of BSA. However, the release of BMP-2 from MCF at pH 6.0 is a little faster than at pH 7.4, which may be attributed to the weaker interaction between positively charged BMP-2 and negatively charged MCF surface at pH 6.0 than at pH 7.4.

To explain whether the conformation and secondary structure of proteins can be maintained, we selected BMP-2 as model protein for measurement. Free BMP-2, BMP-2 released from MCF and MCF-NOCC at pH 6.0 were detected by circular dichroism (CD) spectroscopy, which is one of the most widely used techniques for testing the structure of proteins.[13] As shown in Fig. 4a, the free BMP-2 manifested an intense positive peak at 190 nm and two minus peaks at 200 nm and 218 nm corresponding to α-helix of BMP-2. The protein released from MCF and MCF-NOCC all showed slightly reduced minus peaks, which suggest a decreased α-helix of BMP-2. The secondary structure was evaluated with CDNN V2.1 software and the secondary structure compositions were listed in Table S2. Compared with the free BMP-2, the percentages of α-helix of BMP-2 released from MCF and MCF-NOCC had decreased while the percentages of β-sheets and β-turns were all increased. The changes of folding structure of BMP-2 released from MCF and MCF-NOCC were 12.1% and 5.6%, respectively. It can be demonstrated that the loading and released of BMP-2 from MCF and MCF-NOCC have little effects on the secondary structure of this protein, especially for the MCF-NOCC carrier. The far-UV CD spectra of BSA released from MCF and MCF-NOCC (Fig. S6 and Table S3) showed similar phenomena as the results of BMP-2. The changes of folding structure of BSA released from MCF and MCF-NOCC were 5.7% and 1.8%, respectively.

Furthermore, to examine whether the released BMP-2 can still preserve its bioactivity, we collected BMP-2released from MCF and MCF-NOCC at pH 6.0 at 13 time points within 72 h and mixed them homogeneously. The bioactivity was tested by being cultured with BMSCs and measuring the expression of ALP activity-a noted marker of osteoblast differentiation.[14] It was displayed that BMSCs treated with BMP-2 released from MCF and MCF-NOCC showed a little lower expression of ALP activity than free BMP-2 (Fig. 4b). The histochemical measurement of ALP activity (Fig. 4c) further proved the slightly reduced activity of BMP-2 which released from MCF and MCF-NOCC. Our results demonstrated the hybrid MCF-NOCC ensemble could more effectively maintain the bioactivity of encapsulated proteins. It was reported that, some types of

materials, such as polymer microcapsules, lipids, polypeptide and programmed hydrogels, appear particularly interesting to achieve this goal. Slowing et al.[15] have demonstrated that mesoporous silica with large pore size can effectively retain high bioactivity of enzymes. Furthermore, due to the switching action of NOCC, the encapsulated proteins were separated from the external environment. Therefore, our programmed delivery systems have been proposed as an ideal choice for delivery of protein and maintaining its bioactivity.

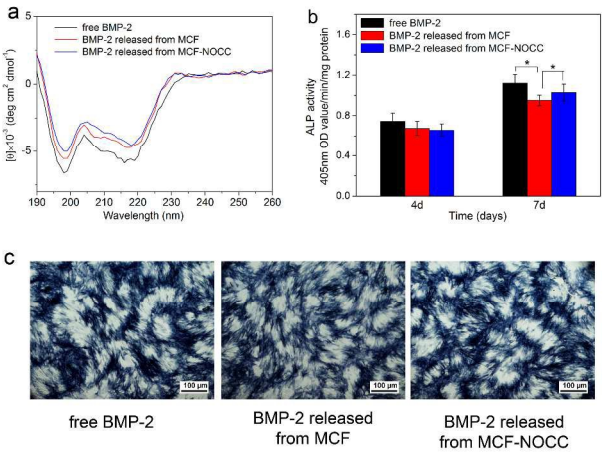

Fig. 4 Bioactivity of the BMP-2 released from MCF and MCF-NOCC. (a) Far-UV CD spectra of free BMP-2 and BMP-2 released from MCF and MCF-NOCC at pH 6.0 (the negative peaks head downward), (b) ALP activity of BMSCs cultured with BMP-2 released from MCF and MCF-NOCC ($n = 5$, $p < 0.05$), (c) ALP activity was histochemically detected by BCIP/NBT ALP Color Development Kit after cultured for 7 days. (Scar bar = 100 μm)

In summary, a pH-responsive NOCC-capped MCF with ultra-large spherical pores and high mesopore volumes was successfully fabricated. This ensemble exhibited a good protein loading. And the encapsulated macromolecules were entrapped in the mesopores in the mimetic normal body fluids (pH 7.4) and quickly released in an acidic environment (pH 6.0). Meanwhile, this hybrid MCF-NOCC could maintain the conformational structure and bioactivity of the encapsulated proteins. It is demonstrated that our new platform represents a promising candidate for future *in vitro* and *in vivo* controlled release of bioactive macromolecules.

The authors wish to express their gratitude to the financial supports from National Basic Research Program of China (973 Program, No. 2012CB933600), the 111 Project (B14018), National Natural Science Foundation of China (No.31470924 and No.31400817), and Chinese Postdoctoral Science Foundation (2013M541484). This study was also supported by Program for New Century Excellent Talents in University (No NCET-11-0640) and the national Special Fund for State Key Laboratory of Bioreactor Engineering (No.2060204).

Notes and references

[a] *The State Key Laboratory of Bioreactor Engineering, East China University of Science and Technology, Shanghai 200237, PR China*
[b] *Key Laboratory for Ultrafine Materials of Ministry of Education, Engineering Research Center for Biomedical Materials of Ministry of Education, East China University of Science and Technology, Shanghai 200237, PR China.*
Email: yyuan@ecust.edu.cn, liucs@ecust.edu.cn
[c] *State Key Laboratory of Chemical Engineering and Department of Chemistry, East China University of Science and Technology, Shanghai 200237, China*

† Electronic Supplementary Information (ESI) available: For all experimental procedures and additional data. See DOI: 10.1039/b000000x/

1. S. Frokjaer and D. E. Otzen, *Nat. Rev. Drug. Discov.*, 2005, **4**, 298-306; H. P. Lim, B. T. Tey and E. S. Chan, *J. Control. Release*, 2014, **186**, 11-21.
2. F. Wan, M. J. Maltesen, S. K. Andersen, S. Bjerregaard, C. Foged, J. Rantanen and M. S. Yang, *Pharm. Res.*, 2014, **31**, 1967-1977.
3. S. R. Choi, D. J. Jang, S. Kim, S. An, J. Lee, E. Oh and J. Kim, *J. Mater. Chem. B*, 2014, **2**, 616-619; S. Ahn, I. H. Lee, E. Lee, H. Kim, Y. C. Kim and S. Jon, *J. Control. Release*, 2013, **170**, 226-232; N. Hammer, F. P. Brandl, S. Kirchhof and A. M. Goepferich, *J. Control. Release*, 2014, **183**, 67-76; J. Seras-Franzoso, K. Peebo, E. Garcia-Fruitos, E. Vazquez, U. Rinas and A. Villaverde, *Acta Biomater.*, 2014, **10**, 1354-1359.
4. H. H. P. Yiu and P. A. Wright, *J. Mater. Chem.*, 2005, **15**, 3690-3700; M. Hartmann, *Chem. Mater.*, 2005, **17**, 4577-4593.
5. B. W. Chen, W. Qi, X. L. Li, C. H. Lei and J. Liu, *Small*, 2013, **9**, 2228-2232; S. Hudson, J. Cooney and E. Magner, *Angew. Chem. Int. Edit.*, 2008, **47**, 8582-8594; X. Du, L. Xiong, S. Dai, F. Kleitz and S. Z. Qiao, *Adv. Funct. Mater.*, 2014, **24**, 7627-7637; X. Du, B. Shi, J. Liang, J. Bi, S. Dai and S. Z. Qiao, *Adv. Mater.*, 2013, **25**, 5981-5985; X. Du, B. Shi, Y. Tang, S. Dai and S. Z. Qiao, *Biomaterials*, 2014, **35**, 5580-5590; A. Popat, J. Liu, G. Q. Lu and S. Z. Qiao, *J. Mater. Chem.*, 2012, **22**, 11173-11178.
6. L. Q. Gu, J. Lim, J. L. Cheong and S. S. Lee, *Chem. Commun.*, 2014, **50**, 7017-7019; X. H. Huang and J. Y. Ying, *Chem. Commun.*, 2007, 1825-1827; J. Lee, J. Kim, S. W. Kim, C. H. Shin and T. Hyeon, *Chem. Commun.*, 2004, 562-563; P. A. Russo, M. Carrott, P. A. M. Mourao and P. J. M. Carrott, *Colloid. Surf. A-Physicochem. Eng. Asp.*, 2011, **386**, 25-35.
7. Q. Gan, X. Y. Lu, Y. A. Yuan, J. C. Qian, H. J. Zhou, X. Lu, J. L. Shi and C. S. Liu, *Biomaterials*, 2011, **32**, 1932-1942; Y. Jia, J. B. Fei, Y. Cui, Y. Yang, L. A. Gao and J. B. Li, *Chem. Commun.*, 2011, **47**, 1175-1177; Y. Lu, W. Sun and Z. Gu, *J. Control. Release*, 2014, **194**, 1-19.
8. J. Wu and M. Sailor, *Adv. Funct. Mater.*, 2009, **19**, 733-741.
9. Y. H. Lin, H. F. Liang, C. K. Chung, M. C. Chen and H. W. Sung, *Biomaterials*, 2005, **26**, 2105-2113.
10. Z. Liu, Y. Jiao and Z. Zhang, *J. Appl. Polym. Sci.*, 2007, **103**, 3164-3168; S. C. Chen, Y. C. Wu, F. L. Mi, Y. H. Lin, L. C. Yu and H. W. Sung, *J. Control. Release*, 2004, **96**, 285-300.
11. S. C. Chen, Y. C. Wu, F. L. Mi, Y. H. Li, L. C. Yu and H. W. Sung, *J. Control. Release*, 2004, **96**, 285-300.
12. T. Crouzier, L. Fourel, T. Boudou, C. Albiges-Rizo and C. Picart, *Adv. Mater.*, 2011, **23**, H111-H118.
13. N. J. Greenfield, *Nat. Protoc.*, 2006, **1**, 2527-2535.
14. Y. Mikami, M. Asano, M. J. Honda and M. Takagi, *J. Cell. Physiol.*, 2010, **223**, 123-133.
15. Slowing, II, B. G. Trewyn and V. S. Y. Lin, *J. Am. Chem. Soc.*, 2007, **129**, 8845-8849.

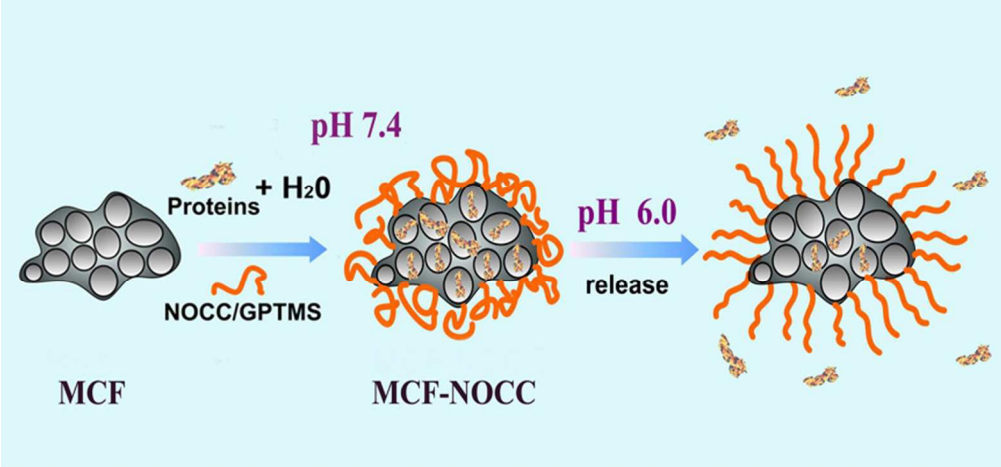

72x34mm (300 x 300 DPI)